Valorising Desalination Brine for Green Cement Production: Toward Mitigating Global CO_2 Emissions

Zhiyuan Zong [1], Omar Daoud [1], Nicholas P. Hankins [1], Qianhong She [2,3] *, Christian D. Peters [1] *

[1] Department of Engineering Science, University of Oxford, Oxford OX1 3PJ, UK

[2] School of Civil and Environmental Engineering, Nanyang Technological University, Singapore 639798, Singapore

[3] Singapore Membrane Technology Centre, Nanyang Environment and Water Research Institute, Nanyang Technological University, Singapore 637141, Singapore

* Corresponding authors:

Qianhong She

Email address: qhshe@ntu.edu.sg

Christian D. Peters

Email address: christian.peters@eng.ox.ac.uk

Abstract

Worldwide, 141.5 million cubic meters of brine are produced by desalination plants per day which is usually rejected and discharged into the ocean without further treatment. Even though some research has been done on brine valorisation, the economic and environmental benefits are rarely understood from a global perspective. This work investigates using desalination brine and low-carbon electricity from renewables as the feedstock in a hybrid process integrating membrane concentration, Chlor-Alkali and mineralisation to produce green MgO cement and other valuable by-products. Under the best practical performance of each individual unit operation, our present-day analysis shows that mitigating CO_2 by brine utilisation has higher economic competitiveness ($48 to $61.8 per metric tonne of CO_2) compared to other CO_2 abatement technologies that are currently available. In addition, the capacity of the proposed process, which is attached to the world's largest seawater desalination plant, can potentially mitigate 5.45 million tons of CO_2 per year. Based on this analysis, it is forecast that, when extrapolated globally with required process tuning based on the regional brine variability, the cement production from the brine utilization process has a theoretical maximum capacity to fulfill up to 14-43% of conventional cement production in 2050. To meet the 2050 net-zero emission goal, utilising rejected desalination brine with green electricity could potentially fulfil up to 47.7% of the global carbon capture sequestration task and mitigate 33.3% to 51.3% of CO_2 from the cement industry, which represents 2.6% to 4% of global CO_2 emissions. This work offers a novel circular economy pathway that transforms desalination brine—a major water industry by-product—into a high-value, low-carbon construction material. The proposed process advances sustainable water management by linking brine treatment with CO_2 mitigation and cement decarbonization.

Keywords:

Brine valorisation, Green Cement, CO_2 mitigation, Carbon abatement cost

1. Introduction

At present, research and development into zero liquid discharge and brine valorisation techniques have shown that the rejected brine in desalination plants can be valorised for the production of sought-after minerals. Sodium, magnesium, and calcium are among the most valuable and plentiful metal ions contained in the rejected brine (Loganathan et al., 2017). Utilising magnesium and calcium from the rejected brine to produce MgO and CaO as a cement binder is also a promising measure to elevate the value of the brine (Dong et al., 2018; Ruan et al., 2021a).

The overall CO_2 emissions from traditional cement production contribute to around 7% of the global CO_2 emission (Benhelal et al., 2013). While broader decarbonization strategies emphasize sector-wide mitigation through emission trading (Hashim et al., 2022) and renewable energy integration (Amirreza et al., 2021), the cement industry demands tailored solutions due to its reliance on carbon-intensive processes. Brine-derived MgO cement bridges this gap by combining CO_2 utilization (e.g., via mineralization, akin to enzymatic approaches (Sharma et al., 2020) with waste valorization, offering a scalable alternative to conventional offsets. Although alternative binders like geopolymers (Nawaz et al., 2020) and Limestone Calcined Clay Cement-LC3 (Sharma et al., 2021) show promise, their feedstock limitations (e.g., fly ash availability) hinder global scalability. Existing MgO production routes, especially the dry route, are energy-intensive and high-emission. In contrast, brine-derived MgO cement leverages abundant desalination byproducts, offering a geographically flexible solution. Recent advances in reactive MgO production (Dong et al., 2018) and CO_2 curing (Wu et al., 2018) demonstrate its technical feasibility but lack integration with upstream brine processing.

Hence, replacing conventional methods of cement production via MgO and CaO cement binder production from brine could become an excellent measure to mitigate CO_2 emissions. Afterwards, the raw cement binder could be sent for further CO_2 curing to enhance its strength (Wu et al., 2018). It could also be a potential method to mitigate CO_2, as the MgO and CaO binder are mineralised in their lifetime by sequestering CO_2 from the atmosphere (Pade and Guimaraes, 2007). Recent studies highlight the potential of membrane-based brine concentration (Wang et al., 2020) and electrochemical NaOH production (Du et al., 2018) to enable circular resource recovery. However, these works focus on isolated unit operations without quantifying system-level CO_2 mitigation potential or economic viability

In the proposed process, the precipitation steps of $Mg(OH)_2$ from brine rely heavily on NaOH. The most famous and widely used process to produce NaOH is by using the chlor-alkali process by electrolyzing high concentration NaCl brine (Thiel et al., 2017). However, the production of NaOH is costly and requires a large amount of electricity. In addition, the high-temperature required for the calcination of $Mg(OH)_2$ to MgO is an energy intensive procedure and requires a certain amount of fuel to support the process. In order to produce cement from brine in a green and more sustainable fashion the development of an energetically more self-sufficient process is required.

Some similar processes have been proposed to produce $Mg(OH)_2$ by utilising the rejected brine. It has been proven by Um et al. that precipitating $Mg(OH)_2$ by NaOH addition is technically viable (Um and Hirato, 2014). The precipitates could be calcinated at high temperatures and dehydrated to MgO. Dong et al. have experimentally validated that $Mg(OH)_2$ can be formed from the rejected brine (Dong et al., 2018). Du et al. have also proposed a reliable

process to produce NaOH from rejected brine (Du et al., 2018).

In this study, a novel, self-sufficient process is presented that only utilises desalination brine and low-carbon electricity for CO_2 mitigation via the production of green cement and additional by-products. The focus is on membrane-based brine concentration, which is energy efficient compared to thermal brine concentrators to allow for conventional NaOH production via the Chlor Alkali process. Both the chemical required for precipitation and the fuel consumed for high temperature precipitation are self-generated. This self-sufficient process has not been proposed in its entirety to date and none of the other presented studies are comprehensive in the sense of showing the global potential for CO_2 mitigation via brine utilisation for cement production.

Many CO_2 mitigation methods are proposed to achieve the 2050 net-zero emission goal. These are primarily divided into two categories: 1) direct carbon capture, sequestration and utilisation, and 2) indirect CO_2 mitigation by shifting the conventional production routes to greener ones. In order to maximize the CO_2 mitigation efficiency, both CO_2 mitigation routes are included in the presented process.

This study starts with the detailed process design from seawater reverse osmosis (SWRO) brine to final products, which include water, MgO cement, hydrogen, and chlorine gas. The detailed technology and environmental analysis exhibit the economic feasibility and the cradle-to-gate carbon footprint of all products. This analysis maps brine availability to cement demand, identifying high-potential regions (e.g., MENA) where SWRO brine composition is consistent (>70% global capacity). The global implication of utilising rejected brine to mitigate global CO_2 emissions and detailed life cycle assessment compared with conventional Portland

cement are proposed in this study. The primary objective of this study is to provide a comprehensive analysis from detailed design to the big picture to arouse the interest and attention to the potential of brine utilisation. The capacity and levelized cost of CO_2 mitigation (LCCM) via brine utilisation will be compared with other more mainstream CO_2 mitigation technologies to show the significant potential of brine utilisation.

2. Materials and Methods

This section outlines the overall framework of the process, with descriptions of selected units within it. The study is based on modeling and analysis, and all modeling software, as well as the economic and environmental parameters used, are detailed in the following section and in the supplementary information.

2.1. Brine utilisation process

The modelled brine utilisation process is shown in **Fig 1**. In this proposed self-sufficient scenario, only two inputs—electricity and brine—are required to produce MgO cement. Additionally, produced water and excess H_2 and Cl_2 gases, after being used for chlorination and fueling the calcination processes, are also considered in the production process.

The rejected brine from the SWRO unit firstly undergoes precipitation to prevent Mg and Ca crystallization in the downstream membrane-based brine concentrator. The discharged brine from the precipitation steps is Na^+-rich but Mg^{2+} lean. OLI Scale Chem 11.0 (OLI System, Inc) is used to calculate the amount of NaOH required to achieve the desired precipitation efficiencies. The proposed process suggests a two-step precipitation to reduce $CaCO_3$ and $Ca(OH)_2$ in the $Mg(OH)_2$ precipitate. $CaCO_3$ primarily precipitates at a pH of 9.0–

147 9.8 (Ruiz-Agudo et al., 2011), while $Mg(OH)_2$ begins to precipitate at pH 9.8 (Vassallo et al.,
148 2021). The first step of precipitation involves raising the solution's pH to 9.8 and using filtration
149 to remove the formed $CaCO_3$. The second step aims to precipitate $Mg(OH)_2$, with the process
150 reaching a final pH of 10.8. In this process, over 99% of magnesium is precipitated. Adding a
151 third precipitation step or increasing the NaOH dosage to recover a higher fraction of
152 magnesium was found to be cost-ineffective due to diminishing precipitation efficiency. A
153 previous pilot-scale study indicated that calcium hydroxide begins to precipitate at a pH of
154 11.75 (Vassallo et al., 2021). Performing precipitation at the proposed pH level helps minimize
155 the co-production of $Ca(OH)_2$ in the commercial magnesium cement product. The precipitated
156 solids, mainly $CaCO_3$ and $Mg(OH)_2$ are sedimented and filtered by ultrafiltration (UF)
157 accordingly, and $Mg(OH)_2$ is dewatered in the filter press for further processing.

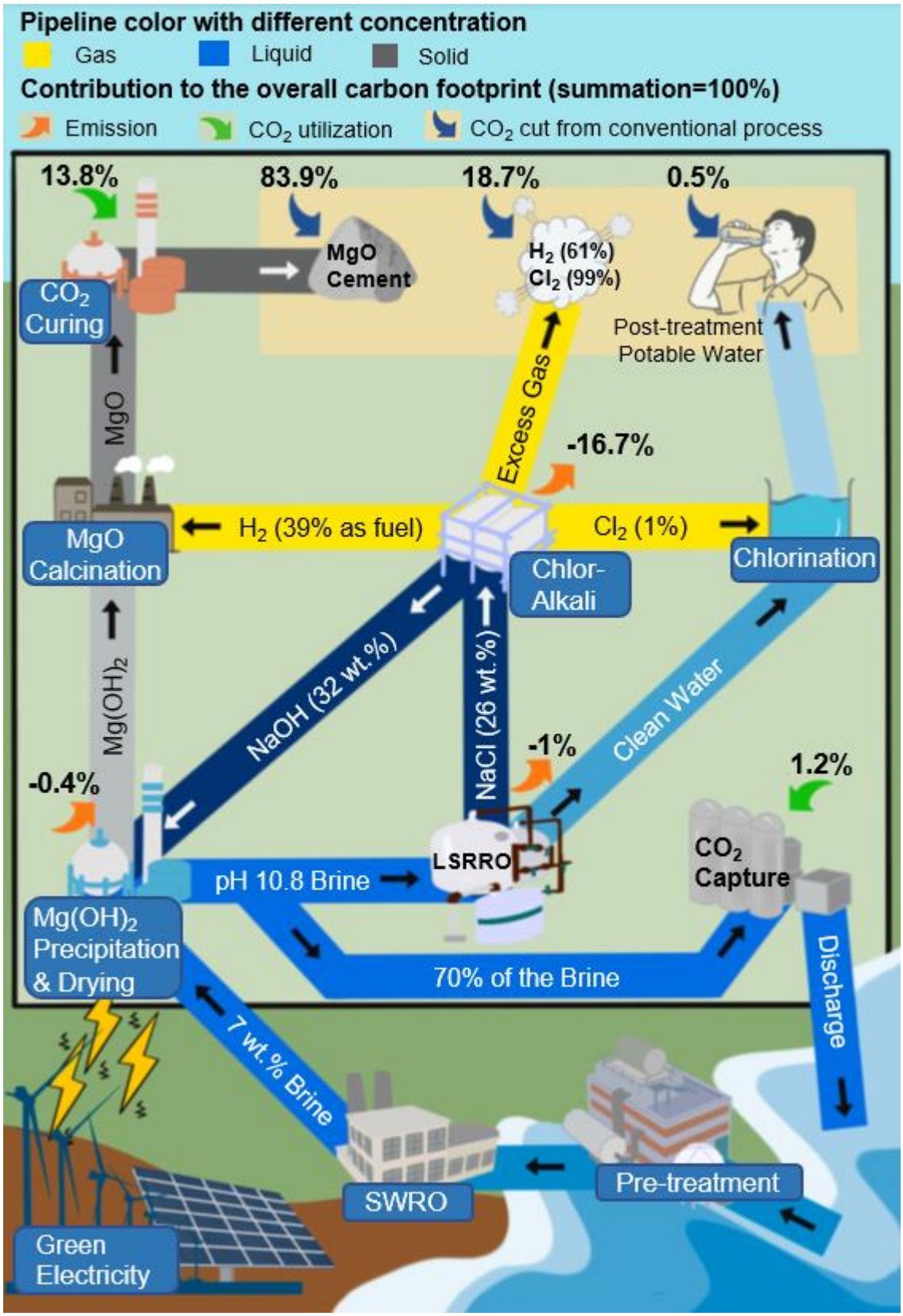

Fig 1. Self-sufficient and CO_2-negative brine utilisation framework (box indicates the suggested and simulated process; yellow zone indicates outputs.)

A fraction of the Na^+-rich brine is then concentrated using a novel membrane process, low salt rejection reverse osmosis (LSRRO). LSRRO is chosen to concentrate the brine stream as it is very energy efficient compared to thermal methods (Wang et al., 2020) while being capable of achieving the required concentration levels required for the chlor-alkali process. The fraction of Na^+-rich brine is concentrated and electrolysed to produce NaOH at the exact required quantities for the former precipitation step, while the rest of the brine is discharged and used for CO_2 capture due to its high pH (Du et al., 2018; Kumar et al., 2021) (Eq.1).

$$2NaCl + 2H_2O = 2NaOH + Cl_2 + H_2 \quad (1)$$

The NaOH production is conducted in a conventional Chlor-Alkali unit. The theoretical electricity consumption of NaOH production with a state-of-the-art Chlor-Alkali unit is 1.56 kWh/kg of NaOH (32 wt%). Considering the efficiency of the electrolyser of 66.6%, 2.35 kWh/kg-NaOH of electricity and additional 0.196 kWh of thermal energy are required under practical operation (Kumar et al., 2021). The practical energy consumption is used in this study.

Along with the NaOH production, the electrolysis process also produces H_2 at the cathode and Cl_2 gas at the anode. Of all the potential electrolysers, the hydrogen generated by the membrane cell has the highest purity (99%) (Erden and Karakilcik, 2024). H_2 is a clean fuel without any greenhouse gas potential. The H_2 is used for preheating the dehydration steps. The co-produced Cl_2 is used for the water chlorination process. Due to the global Covid-19 pandemic, super-chlorination might be necessary (15 mg/L) (Pal, 2017).

The produced precipitates are calcinated in a hydrogen fired heater reactor. The highly endothermic $Mg(OH)_2$ calcination reactions are recommended to operate between 500 °C to 900 °C, respectively (Eq.2&3) (Salomão and Pandolfelli, 2008; Takeuchi et al., 2021; Yang et

al., 2017). The $Mg(OH)_2$ dehydration reaction is designed to operate at low temperature (i.e., 500 °C) to minimize the CO_2 release from $CaCO_3$ calcination, even though the calcinated $CaCO_3$ is very minor. A conservative estimate of the energy efficiency of a state-of-the-art H_2 fired heater is 85%. The dried cement binders are sent to downstream processing for CO_2 curing to enhance the binder strength and sold as cement.

$$Mg(OH)_2 = MgO + H_2O \quad (2)$$

The simulated process is assumed to be attached to the largest membrane desalination plant in the world. The plant's life is assumed to be 25 years in order to analyze the future impact on the 2050 net-zero emission scenarios, and to consider the plant's operating and maintenance costs.

2.2. Economic, environmental and life cycle Analysis

The cost of all pressure-driven devices and the fired heater reactor are generated by CAPCOST (Richard C. Bailie et al., n.d.). The cost of pressure devices depends on their power and discharge pressure, and the cost of the fired heater reactor relies on the duty of the $Mg(OH)_2$ dehydration reaction. The cost of the major equipment (i.e., low-salt-rejection reverse osmosis (LSRRO), chlor-alkali electrolyser, filter press and ultrafiltration units) is obtained by using scaling equations. The detailed scaling methods are listed in section **S2**.

All prices from 2021 were used as a basis for the calculations (i.e., CEPCI 2021) (Jenkins, 2022). All the parameters used in the economic model are assumed on a conservative basis in **Table S1**.

Considering the cost of installation, engineering, piping, and construction, the fixed capital

investment (FCI) of the inside battery limit (ISBL) is usually proportional to the purchased equipment cost depending on the plant type (Sinnott et al., 1999). The factor to summarize FCI is called the Lang factor, Eq (3).

$$FCI = Purchased\ equipment\ cost * Lang\ factor \quad (3)$$

Typically, the Lang factor used for matured large size plant is 6, such as electrolysis (Parkinson et al., 2018; Thomas, 2018). The OSBL (outside battery limit) cost is a factor in the ISBL cost, which includes storage, utility facilities, administrative buildings, and distribution facilities. For a large size plant, the OSBL is assumed to be 40% of the ISBL.

Regarding the operating costs, the utility costs always play an important role. In this brine utilisation process, there are two types of utility streams, namely electricity and the self-produced hydrogen. Therein, electricity is used for the LSRRO brine concentrator, ultrafiltration, filter press and electrolysis. The electricity rate is highly dependent on location and source. Around 50% of the global desalination capacity is located in the Middle East and North African area (MENA) (Jones et al., 2019). High solar irradiance in MENA countries make solar the most likely source of renewable energy within this region. The solar-based electricity rate has dropped to below ¢3/kWh in many areas, such as the USA, Mexico (International Renewable Energy Agency, 2017), and many MENA countries including Oman, Qatar, Saudi Arabia, Bahrain, and the UAE (Apostoleris et al., 2021; Boersma and Griffiths, 2016; Rantissi et al., 2024). ¢3/kWh of electricity rate is also selected in previous Chlor-Alkali research (Roh et al., 2019). Other than solar-based electricity, the International Renewable Energy Agency estimates that electricity from other renewable sources also exhibits high economic competitiveness (Ralon et al., 2017). The electricity price from geothermal,

hydropower, and wind power are down to ¢4, ¢2 and ¢3 per kWh, respectively. The projected wind electricity price is expected to drop further to roughly ¢2/kWh (U.S. Department of Energy, n.d.). In this study, the conservative price of green electricity is used for the base case calculation, which is ¢5/kWh. It is important to note that the electricity rate from renewable sources is set to potentially decrease over the next 30 years (Apostoleris et al., 2018) and significantly benefit the proposed process.

This process benefits from using clean electricity from solar energy in both the environmental and economic analysis. The carbon intensity of solar-based electricity is 51 g-CO_2/kWh in Saudi Arabia (ranging from 14 to 73 g-CO_2/kWh in different countries), which makes the process a low carbon footprint source (Resch, 2007). Because of environmental concerns, carbon tax and credit are widely employed to manage the CO_2 emissions. Carbon trading is being introduced to mitigate global emissions in an economical fashion. Compared to conventional cement and gas production, it is expected that the brine utilisation process would potentially end up with a lower carbon footprint. In this manner, the reduced CO_2 emissions will affect both the environmental and economic aspects. Hence, a conservative carbon tax credit at \$50/t-CO_2 is used for the base case calculation (Parkinson et al., 2018; Zong et al., 2024, 2023a).

The expected revenue is calculated by selling all products at their wholesale prices from their conventional production. Under the discounted cash flow analysis, the required annual revenue is calculated based on the 10% IRR (r) and the Net Present Value (NPV) is zero in 2050, where the C_n indicate the cash flow to achieve the set goal (Hopkinson, 2016).

$$NPV = \sum_{n=0}^{n} \frac{C_n}{(1+r)^t} \quad (4)$$

Hence, the economic penalty is the gap between the required revenue and obtained revenue when selling all the products in their benchmark prices. The economic credit from the desalinated water is not included in the base case scenario but will be discussed in the following sensitivity analysis. The carbon tax credit, (for example, 45V) indicates the credit from the direct CO_2 removal/sequestration from CO_2 capture and curing steps. The economic penalty can be found and used for further analysis.

$$Revenue_{obtained} = \sum Revenue\ (Cement, H_2, Cl\ gas, carbon\ tax\ credit) \quad (5)$$

$$Enconomic\ penalty\ \left(\frac{\$}{kg,cement}\right) = \frac{Revenue_{required} - Revenue_{obtained}}{Mg\ cement\ produced} \quad (6)$$

From an environmental aspect, the carbon footprint of the brine utilisation process is calculated. All the CO_2 mentioned in this study represent CO_2eq, which means all the potential greenhouse gases are included when the CO_2 intensity or abatement is discussed.

$$Carbon\ footprint\ of\ green\ cement\ (\frac{kg,CO_2}{kg,cement}) = \frac{CO_2\ emissions - CO_2\ mitigation}{Mg\ cement\ produced} \quad (7)$$

The carbon emission of the green cement is calculated by summing all emissions generated for the entire process' electricity consumption (kg-CO_2) using solar-based electricity as basis (51 kg-CO_2/kWh, Ecoinvent 3.9).

$$CO_2\ emission\ (kg, CO_2) =$$

$$electricity\ consumption\ (kWh) * carbon\ intensity\ of\ electricity\ (\frac{kg,CO2}{kWh}) \quad (8)$$

To demonstrate the environmental benefit of utilising brine, the CO_2 mitigation is quantified in terms of direct consumption through CO_2 capture and curing, and indirect carbon credit generated from byproducts (eq 9).

$$CO_2\ mitigation, total\ (kg, CO_2)$$

$$= CO_2\ mitigation, direct + CO_2\ mitigation, indirect \quad (9)$$

In the direct CO_2 mitigation component (eq 10), CO_2 capture refers to the absorption of CO_2 by the high-pH brine (modelled by OLI Scale Chem 11.0) to reduce its pH to a level suitable (pH 8) for safe discharge into seawater. Meanwhile, the CO_2 curing component represents the downstream absorption of CO_2 via curing of the produced Mg-based cement, enhancing its strength to the maximum achievable level. According to Wu et al., MgO and CO_2 are mixed at a 1:0.8 molar ratio. To maximize the strength of MgO-based cement, one day of CO_2 curing (0.8 molar ratio, CO_2 to MgO) is recommended where 34% of CO_2 is absorbed (Wu et al., 2018). The further carbonation of cement may negatively impact the durability and cements inherently performance, even though higher CO_2 sequestration could be achieved.

$$CO_2\ mitigation, direct\ (kg, CO_2) = CO_2\ captured + CO_2\ cured \quad (10)$$

Carbon credits from by-products are determined based on their conventional production method using (1) steam methane reforming (SMR) produced hydrogen, i.e., 9 kg-CO_2/kg-H_2 (Ecoinvent 3.9), and (2) reverse osmosis (RO)-produced water, i.e., 4 kWh/m^3-water as reference (Kim et al., 2019) (eq 11-13).

$$CO_2\ mitigation, indirect\ (kg, CO_2)$$

$$= CO_2\ mitigation, H_2 + CO_2\ mitigation, water \quad (11)$$

$$CO_2\ mitigation, H2\ (kg, CO_2)$$

$$= Surplus\ \ H_2\ for\ sale\ (kg, H2) * CO_2\ intensity\ of\ SMR\ based\ H_2\ (\frac{kg,CO2}{kg,H2}) \quad (12)$$

$$CO_2\ mitigation, water\ (kg, CO_2)$$

$$= Distilled\ water\ (kg, water) * CO_2\ intensity\ of\ RO\ based\ water\ (\frac{kg,CO2}{kg,water}) \quad (13)$$

Hence, the reduction in carbon footprint from using brine-based green cement rather than conventional Portland cement (i.e., 0.9 kg-CO_2/kg-cement, Ecoinvent 3.9) is calculated as

below:

$$Environmental\ credit\ \left(\frac{kg, CO_2}{kg, cement}\right)$$

$$= CO_2\ footprint, Green\ cement - CO_2 footprint, conventional\ PC \quad (14)$$

With the economic penalty and environmental credit calculated, the levelized cost of CO_2 mitigation (LCCM) can be calculated (Parkinson et al., 2019). LCCM shows the cost efficiency of the brine utilisation process to mitigate CO_2 from the conventional processes. The LCCM of brine utilisation will be compared to the cost of some green processes and direct CCS technologies to estimate the best economic option to mitigate CO_2.

$$LCCM = \frac{Economic\ penalty}{Environmental\ credit} = \frac{Cash\ flow\ gap}{CO_2\ mitigation} = \frac{\$}{kg,CO2} \quad (15)$$

The life cycle assessment (LCA) process, as delineated by ISO 14044/40 guidelines, comprises four fundamental stages: goal and scope definition, inventory analysis, impact assessment, and results interpretation (ISO, 2006). In this study, the LCA is conducted to analyse the environmental performance of MgO cement produced from rejected desalination brine. The detailed technology and environmental analysis exhibit the economic feasibility and the cradle-to-gate carbon footprint of all products and compared with the cradle-to-gate emission of the benchmarked product, Portland cement. Detailed procedural information is provided in supplementary information section **S3**.

3. Results and discussion

This section presents the detailed process design of the green cement production, along with its corresponding economic and environmental analyses, global-scale assessment, and future projections.

3.1. Green cement from desalination brine

The economic and environmental analysis in this study is centred around a simulated brine utilisation process that is attached to the world's largest membrane desalination plant (Ras Al Khair, Saudi Arabia, 1,636,000 m^3/day, 50% water recovery by RO). These results are then scaled for global brine volumes (Jones et al., 2019) to paint a 2050 scenario of CO_2 mitigation via brine utilisation. The simulated brine valorisation process utilises the rejected brine from the seawater reverse osmosis units (see supplementary information, section **S1-4** for detail). **Fig 1** indicates the CO_2 contribution and mitigation from each process included in the green cement production process and is scalable based on the brine volume intake. The detailed process design, including flowrates, temperatures, heat duties, concentrations, and pH, are displayed in **Fig 2**. The detailed case study is exhibited in the supplementary information S4.

The previous pilot-scale study proved that by adding NaOH, $Mg(OH)_2$ can be precipitated at very high recoveries (over 99%) with a minority of calcite produced as a by-product (Vassallo et al., 2021). For a typical 7% salinity brine and 32 wt% NaOH from a conventional Chlor-Alkali, 34:1 of brine to NaOH ratio (by volume) is recommended to maximize the precipitation efficiency (see **Fig S1**).

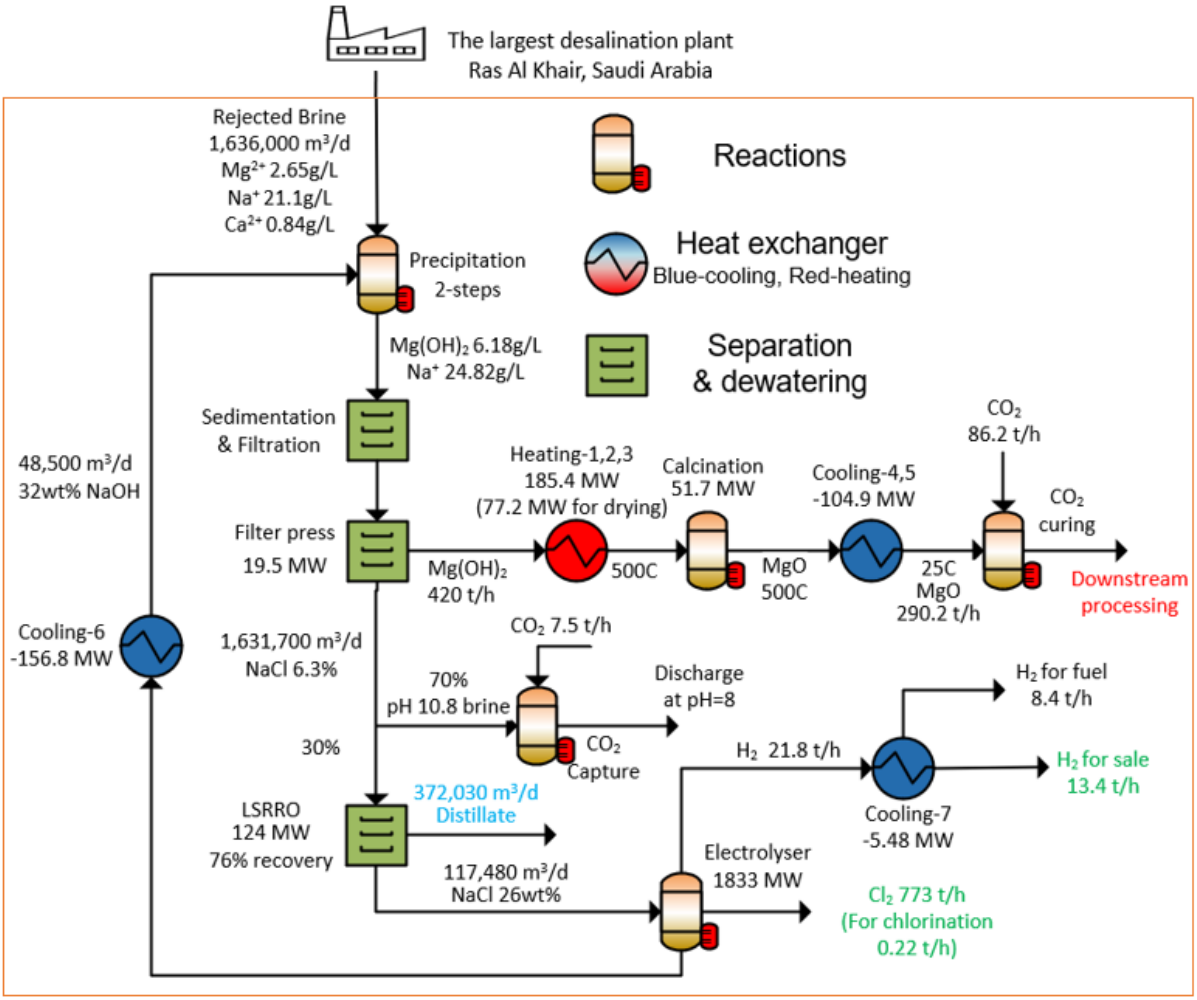

Fig 2. A case study of brine utilisation process attached to the largest desalination plant in the world. The data presented in the process flow diagram is used as the life cycle inventory. The heat integration networks are shown in **Table S3**.

In order to ensure that the brine entering the Chlor-Alkali process has a concentration of 26 wt.% NaCl, LSRRO is used. It is an emerging and energy-efficient technology that is widely applied for the concentration of brine. Compared to conventional mechanical and thermal-based dewatering technology and high-pressure reverse osmosis (HPRO), membrane-based LSRRO can significantly reduce the energy consumption (Davenport et al., 2018) and avoid the use of excessive high hydraulic pressure over 70 bar (Wang et al., 2020). The specific energy consumption is around 8 kWh/m^3 using the four-stage LSRRO to achieve the required brine concentration for the chlor-alkali process (Davenport et al., 2018). Compared to

conventional mechanical and thermal-based dewatering technology and high-pressure reverse osmosis (HPRO), membrane-based LSRRO achieve high water recovery and can significantly reduce the energy consumption (Wang et al., 2020). The brine entering LSRRO is primarily NaCl-rich because the majority of Mg^{2+} and Ca^{2+} have been removed in the previous two-step selective precipitation stage, and significantly less prone to scaling compared to raw SWRO brine. Also, the antiscalant is also common in industrial RO systems (e.g., polyphosphates) to inhibit $CaCO_3$/$Mg(OH)_2$ scaling (Gryta, 2012). Further antifouling measures or periodic chemical cleaning are still suggested based on the site-specific pilot studies (section **S5**) in order to achieve the full-scale implementation (Du et al., 2022).

An alternative membrane process is the semi-close reverse osmosis (SCRO) system which operates at high energy efficiencies and can achieve high recoveries (Mo et al., 2022a). The high recovery can be also achieved efficiently through the hybrid nanofiltration and forward osmosis process (Zong et al., 2023b). However, for this study the chosen concentration process is LSRRO as this process has been studied more widely to date.

As a typical Chlor-Alkali process, 32 wt% of NaOH is produced and used for precipitation. To produce the exact amounts of NaOH for precipitation, 30% of the discharged brine is used and concentrated using the LSRRO, while the rest, 70%, is disposed of at a base case cost. The discharged brine with high pH (10.8) is further utilised for CO_2 capture. The maximum amount of CO_2 capture occurs when the pH of the discharged brine is reduced to 8 again via CO_2 absorption, which matches the pH level of seawater and is safe for discharge. CO_2 captured by the discharged alkaline brine contributes to 1.2% of the overall carbon mitigation. The energy

367 required for drying, preheating and calcination is powered by 39% of the produced hydrogen.
368 A small fraction of the produced Cl_2 is used for water chlorination whereas the rest of the gases
369 are sold. The CO_2 emissions incurred by the LSRRO, electrolysis, filter press and filtration via
370 electricity consumption account for 18.3% of the overall CO_2 mitigated (refer to **Fig 1** and **Fig**
371 **S2d**).

372 The CO_2 mitigated from producing products via their conventional production routes is
373 also considered. 97.7% of CO_2 mitigation from this process originates from 1) the CO_2
374 sequestered in MgO (13.8%) and 2) by avoiding the conventional cement production route of
375 Portland cement (PC) (83.9%). Similarly, circumventing the conventional route of hydrogen
376 production via steam reforming and water production by reverse osmosis contribute to 18.7%
377 and 0.5% of the overall carbon footprint, respectively (refer to **Fig 1**).

378 Reactive MgO hydrates at a similar rate to PC and should not be confused with dead burned
379 MgO. The latter is the result of a much higher calcination temperature, resulting in a much
380 lower reactivity, leading to delayed hydration and cracking, as would be the case for MgO
381 impurities within PC during the clinkering stage (~1450 °C) (Al-Tabbaa, 2013). Synthetic
382 MgO (wet route) expresses higher reactivity compared to commercial MgO. Moreover, it
383 expresses greater compressive strength (Ruan et al., 2021b). The mechanical performance of
384 reactive MgO-based binders plays a pivotal role in evaluating their feasibility as sustainable
385 alternatives to Portland cement (PC). Contrary to concerns associated with MgO-induced
386 expansion in traditional PC systems, brine-derived reactive MgO—produced via low-
387 temperature calcination of precipitated $Mg(OH)_2$—exhibits significantly higher reactivity and
388 finer particle size, enabling early strength development. Reported compressive strengths for

pure reactive MgO binders reach up to 35 MPa at 28 days, comparable to conventional PC (Mo et al., 2019). Furthermore, when blended with PC at substitution levels up to 60%, strengths as high as 80 MPa have been achieved, especially when modified with additives such as ferrous sulfate (Walling and Provis, 2016; Zhang and Panesar, 2019). These performance metrics underscore the engineering viability of brine-based MgO cements. Concerns around dimensional stability and durability can be addressed through optimized curing strategies (e.g., elevated temperature curing and carbonation curing), careful mix design, and incorporation of supplementary cementitious materials. These measures not only mitigate expansion risks but also improve long-term durability, with resistance to sulfate attack and water ingress rivalling or surpassing that of PC-based concretes (Zhang and Panesar, 2019). The further legislation of MgO-based cement is explained in the supplementary information S7. In addition, the estimated CO_2 curing capacity is based on assumptions from the literature and does not account for kinetic or mass transfer limitations during the reaction, which represents a limitation and warrants further research.

The overall calculated CO_2 footprint accounts for any CO_2 emissions (mainly generated indirectly through electricity consumption), any CO_2 consumed during the MgO curing process and through high pH brine sequestration, and the CO_2 mitigated by circumventing conventional production routes of cement and hydrogen. Detailed CO_2 emissions and mitigation data for the studied case are provided in the supplementary information, **Fig S2d**. The world's largest seawater desalination plant has the potential to produce 5084 kilotonnes of commercial Mg-cement annually (section **S4**). The direct and indirect CO_2 that can be mitigated are 820.6 and 1047.5 kilotonnes per year, respectively. The CO_2 emissions of the green cement process would

411 be 989.2 kilotonnes per year due to an hourly electricity consumption of 2214 MWh. Producing
412 one kilogram of green cement using desalination brine (-0.17 kg CO_2/kg cement) achieves a
413 net reduction of 1.07 kg CO_2 compared to conventional Portland cement production, which
414 emits 0.9 kg CO_2 per kilogram (Ecoinvent 3.9). The carbon footprint is 0.04 kg CO_2/kg cement
415 if the CO_2 capture and CO_2 curing steps are excluded.

416 The overall cradle-to-gate environmental benefit of utilising the rejected brine from the
417 largest seawater desalination plant is a total of 5.45 million tonnes of CO_2 mitigated per year
418 (4.63 million tonnes of CO_2 without considering CO_2 curing and capture). To date, the largest
419 CCS plant in the world is the Shute Creek process, located in Wyoming, USA. It captures over
420 7 million tonnes of CO_2 annually (Parker et al., 2011). Utilising the rejected brine would help
421 the largest desalination plant in the world obtain a 78% capacity of the largest CCS plant. A
422 massive benefit of our solution is that it is more scalable than conventional CCS, which requires
423 underground mine/rock formations for CO_2 storage, while the brine utilisation process is less
424 dependent on geology, structure, and hydrology (Kelemen et al., n.d.). The proposed brine
425 utilisation process also has a 5.45 times higher mitigation capacity than the world's largest
426 Direct Air Capture project (IEA, 2021a).

427 To guide future implementation, a four-stage pilot roadmap is proposed (detailed in
428 Supplementary Section S5). This includes: (1) lab-scale integration trials (TRL 3–4, ~6–12
429 months) to validate core operations; (2) CO_2 curing kinetics testing (TRL 3–4, ~6 months) to
430 quantify carbonation performance; (3) bench-scale demonstration (TRL 4–5, ~12–18 months)
431 for continuous flow operation; and (4) a site-coupled pilot plant (TRL 5–6, ~18–24 months)
432 co-located with a desalination facility. These stages will inform system optimization, techno-

433 economic modeling, and environmental validation under real-world conditions.

434

435 ### 3.2. Levelized cost of CO_2 mitigation

436 The case study (section **S4**) shows that if all the products are sold at their conventional
437 market price, the acquired revenue could not meet the production cost and target revenue under
438 the most conservative economic model (the parameters are listed in **Table S1**). With the given
439 economic penalty (revenue gap), and considering the overall CO_2 mitigation potential, the
440 levelized cost of CO_2 mitigation is calculated to be \$61.8/t of CO_2 mitigated. This can be further
441 reduced to \$48/t-CO_2 by including the CO_2 sequestered via brine injection and CO_2 curing of
442 the cement. However, this estimate is based on idealized assumptions and does not account for
443 reactor design factors such as residence time, interfacial area, and mass transfer. It should be
444 interpreted as a theoretical lower bound.

445 Producing cement and hydrogen from desalination brine can significantly contribute to
446 achieving the 2050 net-zero emissions goal set by the United Nations. Compared to many other
447 proposed green processes, utilising desalination brine exhibits a high economic
448 competitiveness. **Fig 3a** shows the CO_2 mitigation cost of different direct or indirect
449 technologies (See section **S6** for detail). In the present-day base case, utilising desalination
450 rejected brine shows the highest economic competitiveness.

451 Many factors affect the CO_2 mitigation cost of the brine utilisation process. The most
452 crucial factor is the electricity cost. The required revenue would equal to the annual expenditure
453 once the electricity rate reduces to $\leq$ ¢2.8/kWh if all the other parameters are kept constant.
454 This means that utilising rejected brine would result in a CO_2 mitigation solution without any

455 extra-economic penalty.

456 Considering both economic penalty and environmental benefit, the base case Levelized
457 Cost of CO_2 Mitigation (LCCM) is 48/t-CO_2. The value would be influenced by many factors.
458 For example, the process also benefits from a lower brine disposal cost. The mitigation cost
459 decreases by $6.2 from the base case, if a previously reported lower brine disposal cost is used
460 ($0.21/$m^3$) (Mo et al., 2022b). The change in product sale prices influence the levelized
461 mitigation cost. When the generated water is sold at $0.8/$m^3$, the mitigation cost is decreased
462 by $19.9/t. In the base case, the hydrogen is sold at gray hydrogen price from steam methane
463 reforming (SMR). According to IEA, the minimum production cost of green hydrogen
464 produced from renewable sources is $3/kg (IEA, 2019). Since the hydrogen is sourced from
465 electrolysis powered by solar-based electricity, green hydrogen prices could be considered, i.e.,
466 $3/kg. This results in the carbon mitigation cost decreasing by $28.1. The critical sale price of
467 hydrogen is $4/kg. When the hydrogen is sold above this price, no economic penalty exists.
468 When the cement and chlorine gas sale price fluctuates by 20%, the mitigation cost varies
469 between $21.9 to $69.7, and, $34.1 to $59.5, respectively. When a process is mature and
470 reaches a higher technology readiness level, a lower expect IRR is required because it shows
471 lower risk (Iloiu and Csiminga, 2009). In order to analyse the maturity effect, IRR varies from
472 7% to 13% were studied. It leads to the LCCM floating significantly from $33.2 to $64.5,
473 which means the TRL could greatly influence the economic competitiveness of brine
474 utilisation.

475 The carbon tax credit varies significantly between different regions, even though it has
476 been introduced globally. On the other hand, the carbon tax credit gradually increases in many

countries. For example, Switzerland's government proposed the highest carbon tax at $130/t (Reuters, 2021). The upper limit of this study analyzes the carbon tax credit at $100 per tonne with free carbon purchase price, whereas the bottom line is no carbon credit with DAC-based CO_2 (**Fig 3b**). The proposed process benefits from high carbon tax credits due to the overall carbon footprint. The mitigation cost varies from $37.4 to $78.1 when the carbon tax credit and carbon purchase price is considered simultaneously.

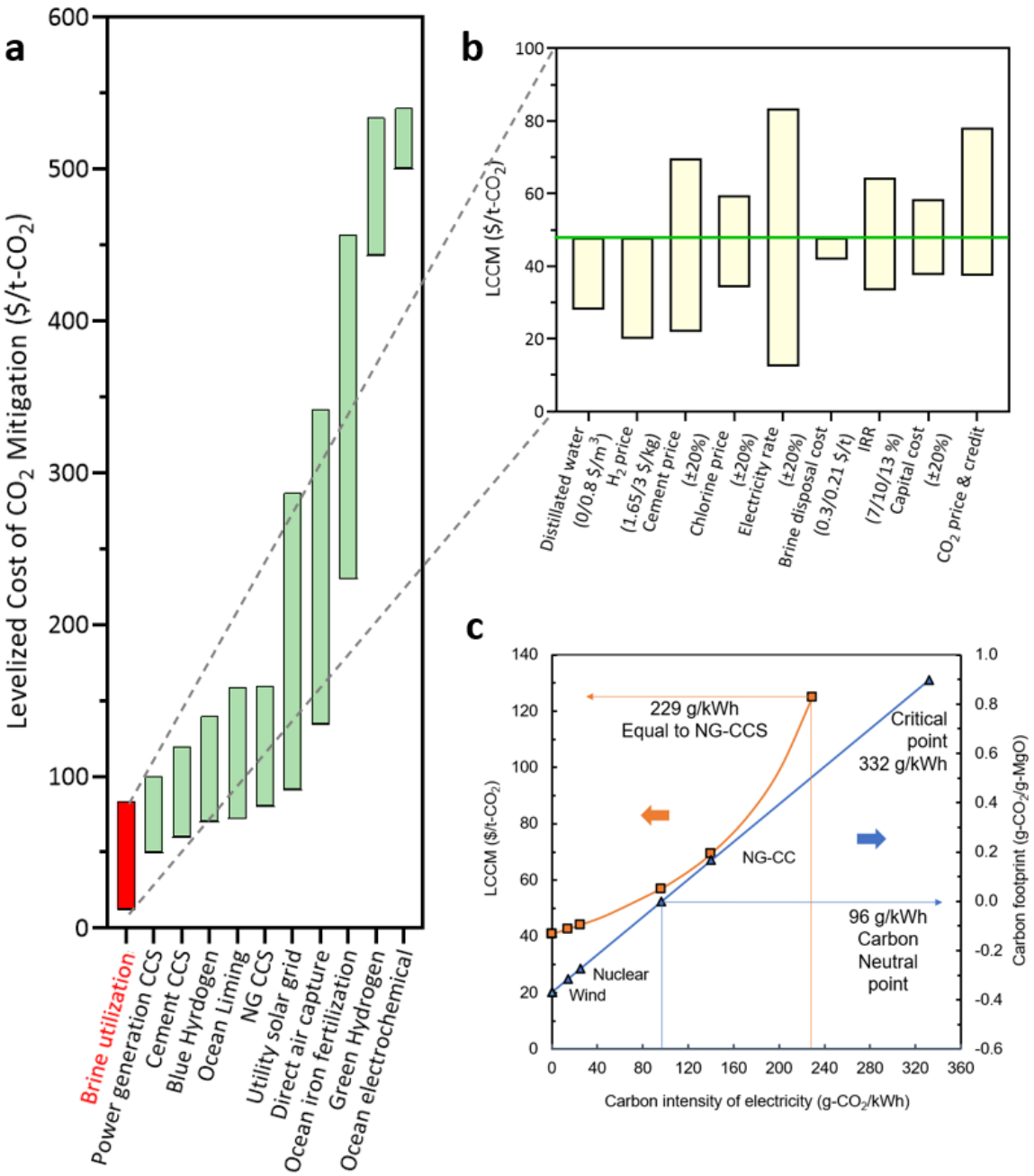

Fig 3. Levelized cost of CO_2 mitigation of brine utilisation process.
(a) CO_2 mitigation cost of mainstream CO_2 mitigation technologies (each comparative process is discussed in section **S6**. The upper and lower limit of the red bar represent the highest and lowest values calculated in 2b)
(b) sensitivity analysis with an NPV of zero and IRR of 10%. The green line indicates the base case scenario of this study and shown in supplementary information. The upper and lower end of CO_2 price & credit bar indicate CO_2 from DAC ($170/t) without carbon credit and free CO_2 source with $100 per tonne of CO_2 credit, respectively.
(c) influence of electricity sources with different carbon intensity

Fig 3b shows how the mitigation cost would be affected under different scenarios. The most influential factor would be the cement sale price. The calcined MgO product could be an alternative for CaO in Portland cement as highlighted in literature given in supplementary information section **S7**. Compared to the conventional PC cement, utilising brine with green electricity would significantly reduce CO_2 emissions by 119% (-0.17 vs 0.9, the breakdown of the CO_2 mitigation was exhibited in **Fig 1**). Because the CO_2 emissions in the proposed process come from electricity generation, the CO_2 footprint and mitigation cost are largely affected by the carbon intensity of the electricity source. Electricity from different sources with different carbon intensities is analyzed. Compared to solar-based electricity, electricity from wind and nuclear exhibits a lower carbon intensity of 14 and 25 g-CO_2/kWh, resulting in a higher mitigation cost ($42.5 and $44) but also a slightly lower carbon footprint (-0.31 and -0.27 t-CO_2/t-cement). The carbon neutral point is reached when the carbon intensity of the electricity source reaches 96 g-CO_2/kWh. Although the process will not sequester carbon above this point, carbon will still be mitigated as the CO_2 emissions are still below that of typical Portland cement (0.9 kg CO_2/kg). This means that the process still mitigates CO_2 emissions if conventional fossil fuel-based electricity sources are used, for example, NG-based electricity with carbon capture (NGCC) (140 g-CO_2/kWh) (Viebahn et al., 2007). CCS costs from a

typical petrochemical process are $125 per tonne (de Coninck and Benson, n.d.). If the carbon intensity of electricity reaches 229 g-CO_2/kWh, the mitigation cost would match the CCS cost of a typical petrochemical process. The critical point is 332 g-CO_2/kWh, which means that when the electricity carbon intensity exceeds this point, the carbon footprint of green cement would exceed that of conventional Portland cement. In order to benchmark the self-sufficient brine-based MgO production, a comparative study to examine the CO_2 emission and energy demand of different MgO production routes is shown in **Table S4**.

3.3. Life cycle assessment results

Fig 4a illustrates the 18-midpoint indicators comparing green cement using mixed NG and solar-based electricity and conventional Portland cement. The purpose of using the mixed electricity sources is to explore the rest 17 environmental impacts, other than CO_2 emissions when the green electricity was not entirely available and the carbon footprint in both cases is equivalent to each other.

Life cycle impacts are primarily driven by energy consumption in green cement production. Green cement exhibits less environmental impact in 10 out of 17 indicators, and one of the indicators show the positive environmental impact, regarding freshwater eutrophication. However, concern arises in the remaining seven environmental indicators, especially stratospheric ozone depletion and marine eutrophication show significant higher impact than Portland cement. These are due to the massive electricity consumption. In general, using conventional electricity from the grid makes the base case process less favourable than Portland cement, whereas mixed electricity shows considerable advantages. Clean electricity,

such as solar electricity, is the most favourable and reduces the impacts over 99% in CO_2 emission and resources, and over 50% in human health and ecosystem, compared to Portland cement (see section **Fig S3** for detailed description). Producing Portland cement via solar-based electricity would also help mitigate the environmental impact by roughly 10%. However, if clean electricity is available, green cement still has an absolute advantage in all categories. If the NG-based electricity is used, that CO_2 emission and three-endpoint factor would result in at least 70% higher than Portland cement **Fig 4b**.

The environmental potential of using NG-based electricity to support green cement production in case green electricity is not available is also explored (**Fig 4c)**. Green cement is more favourable than Portland cement by incorporating either (a) an electrolyzer with improved efficiency (30% electricity reduction or higher) without carbon capture, (b) or at least 30% electricity decarbonization by the suitable CCS technologies with the conventional electrolyser (Chlor-alkali used in **Fig 1**). Both measurements are easy to achieve because both the typical carbon capture rate for standard NGCC power plants (90% CCS (IEA, 2020)) and using alternative energy-efficient electrolyser with lower SEC (Kumar et al., 2021) instead of chlor-alkali (2.35 kWh/kg-NaOH experimentally) are far beyond these thresholds. Hence, green cement production is suitable for a wide range of moderate improvements to carbon capture and electrolyser. It is worth noting that the importance of future work considering long-term carbonation and end-of-life stages for a more holistic environmental assessment.

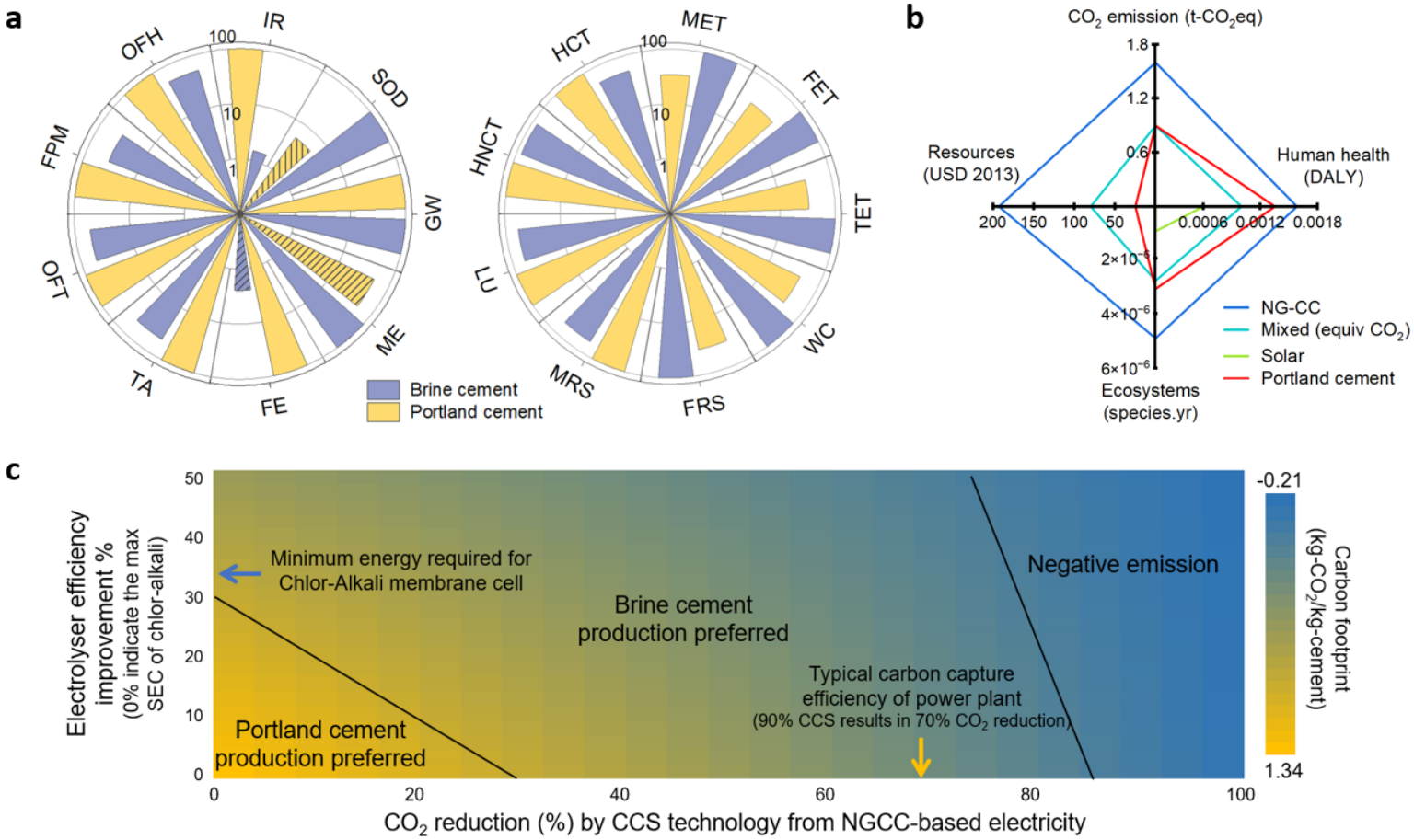

Fig 4. Life cycle assessment comparison of Portland cement and green cement.
(a) Normalized environmental comparison of 18-midpoints categories using mixed electricity at equivalent carbon footprint (dashed-bar indicate positive environmental impact. The abbreviations are shown in table of nomenclature and supplementary information **Table S2**). **(b)** GHG emission and 3-endpoint environmental categories using electricity from different sources. **(c)** Environmental optimization of green cement and Portland cement using natural gas combined cycle (NGCC)-based electricity with carbon capture and sequestration (CCS) and improved electrolyser efficiency. (CO_2 capture and curing are excluded in **b** and **c**)

3.4. Global impact on 2050 net-zero emissions goal

Brine utilisation exhibits a massive potential in the near future and is economically and environmentally competitive. The CO_2 intensity of electricity is one of the main control factors that affect the overall environmental competitiveness, and the critical point mentioned before is 332 g-CO_2/kWh. **Fig 5a** presents the viability of the brine utilisation process in the present-day situation. Concerning the present-day CO_2 intensity of each country in the world, 68 out of the total 195 countries in the world produce electricity with a carbon intensity lower than the critical point. More than half of the countries in Europe (geothermal, nuclear, wind), Africa (solar) and South America (solar, wind) show excellent performance on CO_2 mitigation by taking advantage of their low emission electricity. For example, geothermal-based and hydro-based electricity is widely applied in Iceland and Sweden, emitting only 28.6 and 45.8 g-CO_2/kWh, respectively. This results in an overall carbon footprint of -0.26 and -0.19 t-CO_2/t-cement if produced in these countries, which is a 129% and 121% lower emission compared to the conventional PC cement, respectively. Besides SWRO, many inland countries would also take advantage of valorising saline brines being discharged from brackish and underground desalination plants (Brady et al., 2005; Tang et al., 2021). Utilising inland desalination may result in a higher available brine capacity than calculated in this study, even though the effect of the changes in brine composition would need to be further explored.

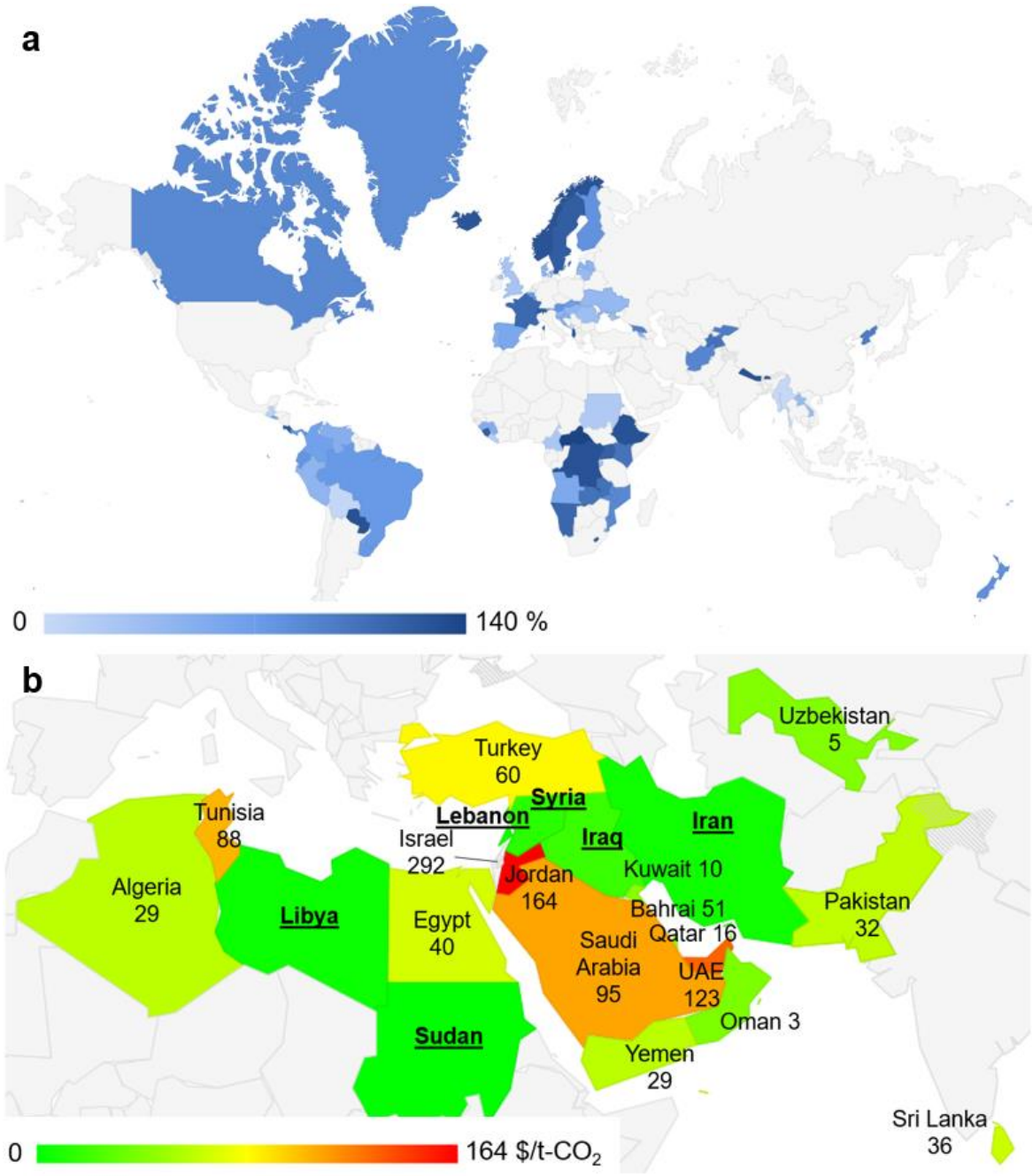

Fig 5. A global outlook of brine utilisation.

(a) Percentage reduction of CO_2 emission by green cement compared to current Portland cement industry. The key variable is the up-to-date carbon intensity of electricity in different countries. 0% indicates the same carbon intensity as conventional Portland cement regarding 0.9 kg-CO_2/kg-cement, and 100% indicate completed decarbonized compared to Portland cement regarding 0 kg-CO_2/kg-cement, number that above 100% indicate negative emissions. **(b)** Levelized cost of CO_2 mitigation in the most desalination-dependent countries when solar-based green electricity (avg 0.051 kg-CO_2/kWh is used) is available. The bold-underlined countries show no economic penalty for CO_2 mitigation, i.e. <$0 per tonne of CO_2. The key variables are the electricity rate and the carbon tax credit in different countries (Supplementary section **S8**).

591 The brine utilisation process can become more applicable and contribute to the 2050 net
592 zero emission goals. This prospect is derived from more and more available clean electricity
593 facilities installed worldwide. The world average CO_2 intensity of electricity generation shows
594 a continuous drop and had an overall 10.4% drop in the past ten years. The localized economic
595 competitiveness of brine utilisation needs to be addressed when green electricity becomes more
596 widely available. With the available green electricity, the levelized cost of CO_2 mitigation is
597 studied by integrating the up-to-date electricity price and carbon tax credit. **Fig 5b** shows the
598 LCCM in the Middle East and North Africa (MENA) and the top 20 most water-stressed
599 countries. The water-stressed countries are usually located in arid areas with the potential for
600 abundant solar electricity. Due to these solar sources, the electricity rate in MENA and the most
601 water-stressed countries typically exhibit the most affordable prices around the world, which
602 further benefits the LCCM from brine utilisation. In addition, potable water in the MENA
603 countries is largely produced via desalination, which produces a large brine capacity in these
604 countries (Jones et al., 2019). Generally, there is a positive correlation between desalination
605 capacity and LCCM from brine utilisation. Compared to the top 20 GDP entities **(Fig S4)**,
606 MENA and other water-stressed countries exhibit significantly lower LCCM from brine
607 utilisation. Those water-stressed countries could spearhead CO_2 mitigation via brine
608 valorisation once renewable energy sources have a greater contribution to the country's energy
609 mix.

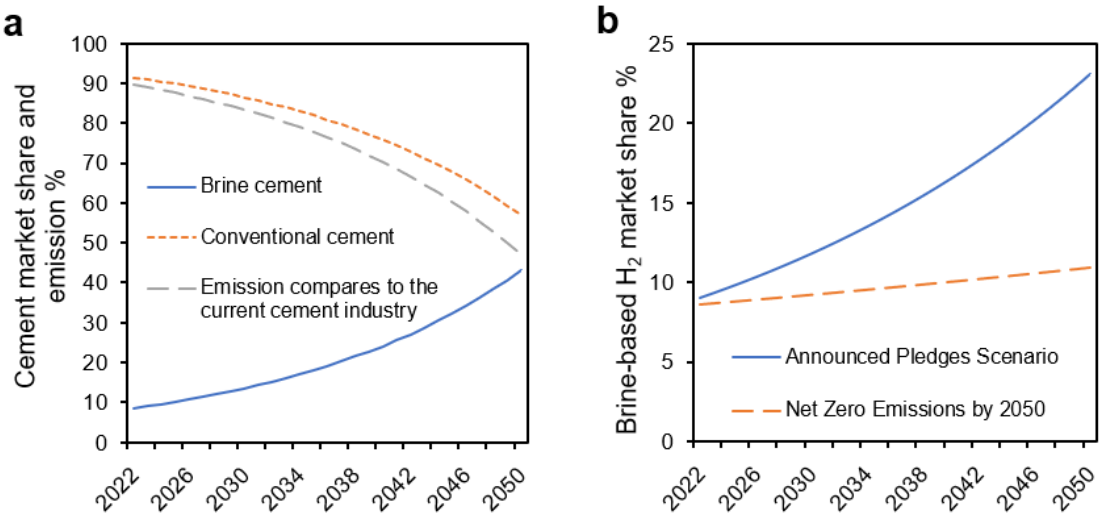

Fig 6. Forecast of brine utilisation in 2050 net zero scenario.
(a) Cement industry emission as a percentage of the current cement industry and market share **(b)** hydrogen production market share under different scenarios

Brine utilisation also has a significant CO_2 mitigation capacity. With the brine utilisation plant retrofitted, the largest desalination plant potentially appears in the top 20 CCS projects worldwide. According to IEA (IEA, 2013), the projected CCS project capacity will reach 1,000 million tonnes annually in 2025. By scaling up the presented process to the worldwide desalination capacity (5.45 million tonnes mitigated by the proposed process attached to the largest desalination plant means 477 tonnes mitigated globally) (Jones et al., 2019), the CO_2 mitigated from brine utilisation would undertake around 47.7% of global CCS tasks (1000 million tonnes per year) if 100% of all desalination brine is utilised.

Brine utilisation, both economically and environmentally, affects the cement and hydrogen industries. **Fig 6** presents the forecast for the cement and hydrogen industries to 2050. Currently, brine-based cement could supply 7% of the global cement market if brine from all global desalination plants is utilised. IEA's report shows that cement production increased annually by 1.8% from 2015 to 2020 (IEA, 2021b), and the desalination capacity will rise more

628 rapidly at 7% per year (Eke et al., 2020). IEA also proposed that the clinker to cement ratio
629 should decrease annually by 0.8% from currently 0.66 in order to meet the 2050 net-zero goal
630 (IEA, 2021b). Assuming the increasing rate of cement production and desalination capacity
631 will continue to 2050, the market share of brine-based cement could gradually reach 43% by
632 2050 under the theoretical maximum scenario (14% if only SWRO brine is used). Meanwhile,
633 up to 51.3% of the CO_2 emission from the cement industry can be mitigated in 2050,
634 representing 4% of the global CO_2 emission. However, some potential regional constraints
635 should be considered, such as coastal nations with limited desalination and landlocked
636 countries without desalination capacity. The proposed process is more feasible to be adapted
637 in the coastal nations with >1,000 MLD desalination (Jones et al., 2019), which covers 65% of
638 global brine supply. As a result, the conservative analysis shows 33.3% cement CO_2
639 mitigation (2.6% of global CO_2) is achievable in feasible regions, and the global 51.3%
640 mitigation requires breakthroughs in brine logistics and would be the upper bound mitigation.
641 This projection value exhibits the theoretical maximum and assumes priority deployment
642 in SWRO-dominated regions (MENA, Mediterranean, etc.), where brine composition is
643 relatively consistent. Even though the SWRO constitutes the majority (>70%) of global
644 desalination capacity (Jones et al., 2019), the necessary process tuning is required due to the
645 regional brine variability. In addition, while brine-derived MgO cement offers a promising
646 decarbonization route, it will compete with other emerging low-carbon cement formulations
647 such as LC3 (Sharma et al., 2021), geopolymers (Nawaz et al., 2020), and carbonated calcium
648 silicates (Ren et al., 2024). Each of these technologies has distinct regional advantages and no
649 single solution is expected to achieve >40% market share in practice, which means a diversified

portfolio of solutions will likely be needed to decarbonize the global cement industry.

The annual hydrogen demand under announced pledges and net-zero emission scenarios are 250 and 530 million tonnes, respectively (IEA, 2021c). Electrolysis of the rejected brine would supply 23.1% and 10.9% of the hydrogen demand under the two different scenarios.

4. Conclusions

This study demonstrates the substantial potential of a self-sufficient process to convert desalination brine into green magnesium cement and other valuable by-products, leveraging low-carbon electricity. The novelty of this work lies in its integration of desalination brine valorization with MgO cement production using a fully modeled process chain—encompassing membrane concentration, chlor-alkali electrolysis, reactive MgO calcination, and CO_2 curing—combined with a cradle-to-gate life cycle and techno-economic assessment. The proposed process not only addresses the environmental challenge of brine disposal but also offers an economically viable and scalable solution for CO_2 mitigation.

By achieving competitive costs as low as \$48 per tonne of CO_2 abatement—significantly lower than conventional direct air capture systems (\$100–\$600/t-CO_2)—and demonstrating the potential to mitigate over 5 million tonnes of CO_2 annually when integrated with a large desalination plant, this approach proves both economically and environmentally advantageous compared to other green cement alternatives. Furthermore, the process enables valorization of wide range of global brine waste, demonstrating clear potential for impact in both water treatment and construction sectors. These findings contribute to bridging water-energy-materials interconnections in sustainable infrastructure development. The integration of this

process on a global scale could significantly reduce CO_2 emissions from the cement industry and contribute to achieving net-zero emission goals by 2050. When extrapolated globally, the proposed process has a theoretical maximum capacity to fulfill up to 43% of 2050 cement demand and mitigate up to 4% of global CO_2 emissions, positioning it as a competitive alternative to emerging green cement technologies such as LC3 and geopolymers.

Although promising, MgO-based cement systems face technical challenges that require further investigation, particularly related to long-term durability, including excessive carbonation, limited water resistance, and expansion due to delayed brucite formation. These factors must be carefully managed through curing protocols, mix design, and material optimization before widespread replacement of Portland cement.

Looking forward, several avenues for improvement and further research can enhance the feasibility and sustainability of this process. Energy efficiency remains a key area for optimization; integrating alternative technologies or improving the energy storage systems could reduce the reliance on large electricity inputs. Additionally, optimizing the flow of the process to minimize liquid discharge could enhance overall efficiency and environmental performance. Variability in brine composition across different desalination plants worldwide may introduce challenges; future studies should explore how location-specific factors affect the performance and output of the process to establish standardized protocols. Ensuring a consistent supply of green electricity is essential to maintain the low-carbon footprint of the process, which underscores the importance of advancing renewable energy technologies and grid stability. Future research should also focus on pilot-scale demonstrations to validate full-system integration and operability. While CO_2 curing is central to carbon sequestration and

694 strength development, this study does not include kinetic or mass transfer modeling, which is
695 a key limitation. Future work should experimentally validate CO_2 uptake rates, curing duration,
696 and carbonation depth. Particular attention is also needed to assess membrane fouling and
697 scaling under continuous operation and to evaluate the process performance across a range of
698 brine compositions, including inland, brackish, and wastewater-derived streams. By addressing
699 these constraints and opportunities, the proposed process can pave the way for a more
700 sustainable and economically viable future for both the desalination and cement industries.
701
702

Nomenclature

Abbreviation or Symbol	Full Name	Unit (if applicable)
CCS	Carbon capture and sequestration	
C*n*	Cash flow	$
DAC	Direct air capture	
FCI	Total fixed capital investment	$
IRR	Internal rate of return	
ISBL	Inside battery limit	
LCCM	Levelized cost of CO_2 mitigation	$/kg-$CO_2$
LSRRO	Low salt rejection reverse osmosis	
NGCC	Natural gas combined cycle	
NPV	Net present value	$
OSBL	Outside battery limit	
PC	Portland cement	
SCRO	Semi-close reverse osmosis	
SMR	Steam methane reforming	
SWRO	Seawater reverse osmosis	
t	Time (year)	

Note: This table lists general terms.

LCA Nomenclature	Midpoint Environmental Impact	Unit (if applicable)
FE	Freshwater eutrophication	kg P eq
FET	Freshwater ecotoxicity	kg 1,4-DCB
FPM	Fine particulate matter formation	kg PM2.5 eq
FSS	Fossil resource scarcity	kg oil eq
GW	Global warming	kg CO_2eq
HCT	Human carcinogenic toxicity	kg 1,4-DCB
HNCT	Human non-carcinogenic toxicity	kg 1,4-DCB
IR	Ionizing radiation	kBq Co-60 eq
LU	Land use	m^2a crop eq
ME	Marine eutrophication	kg N eq
MET	Marine ecotoxicity	kg 1,4-DCB
MRS	Mineral resource scarcity	kg Cu eq
OFH	Ozone formation, Human health	kg NOx eq
OFT	Ozone formation, Terrestrial ecosystems	kg NOx eq
SOD	Stratospheric ozone depletion	kg CFC11eq
TA	Terrestrial acidification	kg SO_2 eq
TET	Terrestrial ecotoxicity	kg 1,4-DCB
WC	Water consumption	m^3

Note: This table is specific to LCA (Life Cycle Assessment).

709

Calculation Terms	Description	Unit (if applicable)
CO_2 mitigation, direct	CO_2 mitigation from direct CO_2 capture by brine and MgO curing of the studied process	kg-CO_2
CO_2 mitigation, indirect	CO_2 credit from byproduct due to the avoidance the CO_2 emission from their conventional production method	kg-CO_2
CO_2 mitigation, H_2	CO_2 credit from surplus hydrogen due to the avoidance the CO_2 emission from steam methane reforming routes	kg-CO_2
CO_2 mitigation, water	CO_2 credit from distilled water due to the avoidance the CO_2 emission from reverse osmosis routes	kg-CO_2
CO_2 mitigation, total	The overall CO_2 mitigation including both direct and indirect portions	kg-CO_2
CO_2 emissions	The overall CO_2 emission from electricity that consumed via the studied process	kg-CO_2
CO_2 footprint, green cement	The overall carbon intensity of green cement base on the studied process	kg-CO_2/kg-cement
Economic penalty	The revenue gap between the required revenue and obtained revenue per kg of cement	$/kg-cement
Environmental credit	The CO_2 footprint difference between green cement and conventional Portland cement	kg-CO_2/kg-cement
Levelized cost of CO_2 mitigation (LCCM)	The extra economic cost to mitigate per unit mass of CO_2 via the proposed green cement process	$/kg-$CO_2$
Revenue, obtained	Revenue acquired if selling all the product under the base case price	$
Revenue, required	Revenue required to achieve the set economic goal (NPV=0, IRR=10%)	$

710 *Note: This table includes terms used in Section 2.2 calculations.*
711
712
713
714
715
716
717

Supplementary materials

Supplementary material associated with this article can be found, in the online version, at doi: xxx

Acknowledgements

Zhiyuan Zong gratefully acknowledges the support of St. Anne's College, University of Oxford, through the MCR Grant and Graduate Research Grant.

Author Contributions

Zhiyuan. Zong: Conceptualization, Methodology, Investigation, Data curation, Formal analysis, Writing - original draft, Writing – review & Editing.
Omar Daoud: Investigation, Writing - original draft
Nicholas P. Hankins: Writing - review & editing, Supervision.
Qianhong. She: Methodology, Investigation, Formal analysis, Writing - review & editing, Supervision.
Christian D. Peters: Conceptualization, Methodology, Investigation, Formal analysis, Writing - review & editing, Supervision

Competing interest

The authors declare that they have no known competing financial interests or personal relationships that could have appeared to influence the work reported in this paper.

Data availability

Data will be made available upon reasonable request via the corresponding authors.

References

Al-Tabbaa, A., 2013. Reactive magnesia cement, in: Eco-Efficient Concrete. Elsevier Ltd., pp. 523–543. https://doi.org/10.1533/9780857098993.4.523

Amirreza, N., Zulkurnain, A.-M., Naveed, A.R., Hesam, K., Shreeshivadasan, C., Veeramuthu, A., Jalal, T., 2021. Assessment of carbon footprint from transportation, electricity, water, and waste generation: towards utilisation of renewable energy sources. Clean Technol Environ Policy 23, 183–201.

Apostoleris, H., al Ghaferi, A., Chiesa, M., 2021. What is going on with Middle Eastern solar prices, and what does it mean for the rest of us? Prog Photovolt 29, 638–648. https://doi.org/10.1002/pip.3414

Apostoleris, H., Sgouridis, S., Stefancich, M., Chiesa, M., 2018. Evaluating the factors that led to low-priced solar electricity projects in the Middle East. Nat Energy 3, 1109–1114. https://doi.org/10.1038/s41560-018-0256-3

Benhelal, E., Zahedi, G., Shamsaei, E., Bahadori, A., 2013. Global strategies and potentials to curb CO2 emissions in cement industry. J Clean Prod 51, 142–161. https://doi.org/10.1016/J.JCLEPRO.2012.10.049

Boersma, T., Griffiths, S., 2016. Reforming energy subsidies: Initial lessons from the United Arab Emirates. Brookings Security and Climate Initiative/Masdar Institute.

Brady, P. v, Kottenstette, R.J., Mayer, T.M., Hightower, M.M., 2005. Inland desalination: challenges and research needs. J Contemp Water Res Educ 132, 46–51.

Davenport, D.M., Deshmukh, A., Werber, J.R., Elimelech, M., 2018. High-Pressure Reverse Osmosis for Energy-Efficient Hypersaline Brine Desalination: Current Status, Design Considerations, and Research Needs. Environ Sci Technol Lett 5, 467–475. https://doi.org/10.1021/acs.estlett.8b00274

de Coninck, H., Benson, S.M., n.d. Carbon Dioxide Capture and Storage: Issues and Prospects. Annu Rev Environ Resour 39, 243–270. https://doi.org/10.1146/annurev-environ-032112-095222

Dong, H., Unluer, C., Yang, E.H., Al-Tabbaa, A., 2018. Recovery of reactive MgO from reject brine via the addition of NaOH. Desalination 429, 88–95. https://doi.org/10.1016/J.DESAL.2017.12.021

Du, F., Warsinger, D.M., Urmi, T.I., Thiel, G.P., Kumar, A., Lienhard V, J.H., 2018. Sodium Hydroxide Production from Seawater Desalination Brine: Process Design and Energy Efficiency. Environ Sci Technol 52, 5949–5958. https://doi.org/10.1021/acs.est.8b01195

Du, Y., Wang, Z., Cooper, N.J., Gilron, J., Elimelech, M., 2022. Module-scale analysis of low-salt-rejection reverse osmosis: Design guidelines and system performance. Water Res 209, 117936. https://doi.org/10.1016/J.WATRES.2021.117936

Eke, J., Yusuf, A., Giwa, A., Sodiq, A., 2020. The global status of desalination: An assessment of current desalination technologies, plants and capacity. Desalination 495, 114633. https://doi.org/10.1016/j.desal.2020.114633

Erden, M., Karakilcik, M., 2024. Experimental investigation of hydrogen production performance of various salts with a chlor-alkali method. Int J Hydrogen Energy 52, 546–560. https://doi.org/10.1016/J.IJHYDENE.2023.08.049

Gryta, M., 2012. Polyphosphates used for membrane scaling inhibition during water desalination by membrane distillation. Desalination 285, 170–176. https://doi.org/10.1016/J.DESAL.2011.09.051

Hashim, H., Zubir, M.A., Kamyab, H., Zahran, M.F.I., 2022. Decarbonisation of the industrial sector through greenhouse gas mitigation, offset, and emission trading schemes. Chem Eng Trans 97, 511–516.

Hopkinson, M., 2016. Net present value and risk modelling for projects, Advances in project management. Lobdon ; New York.

IEA, 2021a. Direct Air Capture. Paris.

IEA, 2021b. Cement. Paris.

IEA, 2021c. Global Hydrogen Review. Paris.

IEA, 2020. Today in the Lab – Tomorrow in Energy? Paris.

IEA, 2019. The Future of Hydrogen. Paris.

IEA, 2013. Technology Roadmap - Carbon Capture and Storage 2013. Paris.

Iloiu, M., Csiminga, D., 2009. Project risk evaluation methods-sensitivity analysis. Annals of the University of Petrosani, Economics 9, 33–38.

International Renewable Energy Agency, 2017. Renewable Energy Auctions: Analysing 2016.
ISO, I., 2006. ISO 14040. Environmental management–Life cycle assessment–Principles and framework (ISO 14040: 2006).
Jenkins, S., 2022. CEPCI annual average value rises precipitously from last year [WWW Document]. URL https://www.chemengonline.com/cepci-annual-average-value-rises-precipitously-from-last-year/
Jones, E., Qadir, M., van Vliet, M.T.H., Smakhtin, V., Kang, S., 2019. The state of desalination and brine production: A global outlook. Sci Total Environ 657, 1343–1356. https://doi.org/10.1016/j.scitotenv.2018.12.076
Kelemen, P., Benson, S.M., Pilorgé, H., Psarras, P., Wilcox, J., n.d. An Overview of the Status and Challenges of CO2 Storage in Minerals and Geological Formations. Frontiers in climate 1. https://doi.org/10.3389/fclim.2019.00009
Kim, J., Park, K., Yang, D.R., Hong, S., 2019. A comprehensive review of energy consumption of seawater reverse osmosis desalination plants. Appl Energy 254, 113652. https://doi.org/10.1016/j.apenergy.2019.113652
Kumar, A., Du, F., Lienhard, J.H., 2021. Caustic Soda Production, Energy Efficiency, and Electrolyzers. ACS Energy Lett 6, 3563–3566. https://doi.org/10.1021/acsenergylett.1c01827
Loganathan, P., Naidu, G., Vigneswaran, S., 2017. Mining valuable minerals from seawater: a critical review. Environ Sci (Camb) 3, 37–53. https://doi.org/10.1039/c6ew00268d
Mo, L., Fang, J., Hou, W., Ji, X., Yang, J., Fan, T., Wang, H., 2019. Synergetic effects of curing temperature and hydration reactivity of MgO expansive agents on their hydration and expansion behaviours in cement pastes. Constr Build Mater 207, 206–217. https://doi.org/10.1016/J.CONBUILDMAT.2019.02.150
Mo, Z., Li, D., She, Q., 2022a. Semi-closed reverse osmosis (SCRO): A concise, flexible, and energy-efficient desalination process. Desalination 544, 116147. https://doi.org/10.1016/J.DESAL.2022.116147
Mo, Z., Peters, C.D., Long, C., Hankins, N.P., She, Q., 2022b. How split-feed osmotically assisted reverse osmosis (SF-OARO) can outperform conventional reverse osmosis (CRO) processes under constant and varying electricity tariffs. Desalination 530, 115670. https://doi.org/10.1016/J.DESAL.2022.115670
Nawaz, M., Heitor, A., Sivakumar, M., 2020. Geopolymers in construction - recent developments. Constr Build Mater 260, 120472. https://doi.org/10.1016/J.CONBUILDMAT.2020.120472
Pade, C., Guimaraes, M., 2007. The CO2 uptake of concrete in a 100 year perspective. Cem Concr Res 37, 1348–1356. https://doi.org/10.1016/j.cemconres.2007.06.009
Pal, P., 2017. Chemical Treatment Technology. Industrial Water Treatment Process Technology 21–63. https://doi.org/10.1016/B978-0-12-810391-3.00002-3
Parker, M.E., Northrop, S., Valencia, J.A., Foglesong, R.E., Duncan, W.T., 2011. CO2 management at ExxonMobil's LaBarge field, Wyoming, USA. Energy Procedia 4, 5455–5470. https://doi.org/10.1016/J.EGYPRO.2011.02.531
Parkinson, B., Balcombe, P., Speirs, J.F., Hawkes, A.D., Hellgardt, K., 2019. Levelized cost of CO2 mitigation from hydrogen production routes. Energy Environ Sci 12, 19–40. https://doi.org/10.1039/C8EE02079E
Parkinson, B., Tabatabaei, M., Upham, D.C., Ballinger, B., Greig, C., Smart, S., McFarland, E., 2018. Hydrogen production using methane: Techno-economics of decarbonizing fuels and chemicals.

Int J Hydrogen Energy 43, 2540–2555. https://doi.org/10.1016/j.ijhydene.2017.12.081
Ralon, P., Taylor, M., Ilas, A., Diaz-Bone, H., Kairies, K., 2017. Electricity storage and renewables: Costs and markets to 2030. International Renewable Energy Agency: Abu Dhabi, United Arab Emirates 164.
Rantissi, T., Gitis, V., Zong, Z., Hankins, N., 2024. Transforming the Water-Energy Nexus in Gaza: A Systems Approach. Global Challenges 2300304.
Ren, M., Shen, P., Tao, Y., Poon, C. sun, 2024. Development of highly carbonation-effective calcium silicates (β-C2S): Phase evolution, microstructure, and carbonation mechanisms. Cem Concr Res 181, 107542. https://doi.org/10.1016/J.CEMCONRES.2024.107542
Resch, R., 2007. The Promise of Solar Energy: A Low-Carbon Energy Strategy for the 21st Century.
Reuters, 2021. After voter slap, Switzerland tries again with plan to slash emissions.
Richard C. Bailie, Debangsu Bhattacharyya, Joseph A. Shaeiwitz, Richard Turton, Wallace B. Whiting, n.d. Analysis, Synthesis, and Design of Chemical Processes, Fourth Edition. Pearson.
Roh, K., Brée, L.C., Perrey, K., Bulan, A., Mitsos, A., 2019. Flexible operation of switchable chlor-alkali electrolysis for demand side management. Appl Energy 255, 113880. https://doi.org/10.1016/J.APENERGY.2019.113880
Ruan, S., Yang, E.-H., Unluer, C., 2021a. Production of reactive magnesia from desalination reject brine and its use as a binder. Journal of CO2 utilization 44. https://doi.org/10.1016/j.jcou.2020.101383
Ruan, S., Yang, E.H., Unluer, C., 2021b. Production of reactive magnesia from desalination reject brine and its use as a binder. Journal of CO2 Utilization 44. https://doi.org/10.1016/j.jcou.2020.101383
Ruiz-Agudo, E., Putnis, C. V, Rodriguez-Navarro, C., Putnis, A., 2011. Effect of pH on calcite growth at constant aCa2+/aCO32-ratio and supersaturation. Geochim Cosmochim Acta 75, 284–296.
Salomão, R., Pandolfelli, V.C., 2008. Magnesia sinter hydration–dehydration behavior in refractory castables. Ceram Int 34, 1829–1834. https://doi.org/10.1016/J.CERAMINT.2007.06.009
Sharma, M., Bishnoi, S., Martirena, F., Scrivener, K., 2021. Limestone calcined clay cement and concrete: A state-of-the-art review. Cem Concr Res 149, 106564. https://doi.org/10.1016/J.CEMCONRES.2021.106564
Sharma, T., Sharma, S., Kamyab, H., Kumar, A., 2020. Energizing the CO2 utilization by chemo-enzymatic approaches and potentiality of carbonic anhydrases: A review. J Clean Prod 247, 119138. https://doi.org/10.1016/J.JCLEPRO.2019.119138
Sinnott, R.K., Coulson, J.M., Richardson, J.F., 1999. Chemical engineering. Vol. 6, Chemical engineering design, 3rd ed. ed, Coulson & Richardson's chemical engineering series. Butterworth-Heinemann, Oxford.
Takeuchi, M., Kurosawa, R., Ryu, J., Matsuoka, M., 2021. Hydration of LiOH and LiCl─ near-infrared spectroscopic analysis. ACS Omega 6, 33075–33084.
Tang, X., Kum, S., Liu, H., 2021. Inland desalination brine disposal: A baseline study from southern California on brine transport infrastructure and treatment potential. ACS ES&T Engineering 2, 456–464.
Thiel, G.P., Kumar, A., Gómez-González, A., Lienhard, J.H., 2017. Utilization of Desalination Brine for Sodium Hydroxide Production: Technologies, Engineering Principles, Recovery Limits, and Future Directions. ACS Sustain Chem Eng 5, 11147–11162.

https://doi.org/10.1021/acssuschemeng.7b02276
Thomas, H., 2018. Options for producing low-carbon hydrogen at scale.
Um, N., Hirato, T., 2014. Precipitation behavior of Ca(OH)2, Mg(OH)2, and Mn(OH)2 from CaCl2, MgCl2, and MnCl2 in NaOH-H2O solutions and study of lithium recovery from seawater via two-stage precipitation process. Hydrometallurgy 146, 142–148. https://doi.org/10.1016/J.HYDROMET.2014.04.006
U.S. Department of Energy, n.d. Advantages and Challenges of Wind Energy [WWW Document]. URL https://www.energy.gov/eere/wind/advantages-and-challenges-wind-energy (accessed 2.22.22).
Vassallo, F., La Corte, D., Cancilla, N., Tamburini, A., Bevacqua, M., Cipollina, A., Micale, G., 2021. A pilot-plant for the selective recovery of magnesium and calcium from waste brines. Desalination 517, 115231. https://doi.org/10.1016/J.DESAL.2021.115231
Viebahn, P., Nitsch, J., Fischedick, M., Esken, A., Schüwer, D., Supersberger, N., Zuberbühler, U., Edenhofer, O., 2007. Comparison of carbon capture and storage with renewable energy technologies regarding structural, economic, and ecological aspects in Germany. International Journal of Greenhouse Gas Control 1, 121–133. https://doi.org/10.1016/S1750-5836(07)00024-2
Walling, S.A., Provis, J.L., 2016. Magnesia-based cements: a journey of 150 years, and cements for the future? Chem Rev 116, 4170–4204.
Wang, Z., Deshmukh, A., Du, Y., Elimelech, M., 2020. Minimal and zero liquid discharge with reverse osmosis using low-salt-rejection membranes. Water Res 170, 115317. https://doi.org/10.1016/J.WATRES.2019.115317
Wu, H.-L., Zhang, D., Ellis, B.R., Li, V.C., 2018. Development of reactive MgO-based Engineered Cementitious Composite (ECC) through accelerated carbonation curing. Constr Build Mater 191, 23–31. https://doi.org/10.1016/j.conbuildmat.2018.09.196
Yang, W., Zhu, Z., Shi, J., Zhao, B., Chen, Z., Wu, Y., 2017. Characterizations of the thermal decomposition of nano-magnesium hydroxide by positron annihilation lifetime spectroscopy. Powder Technol 311, 206–212. https://doi.org/10.1016/J.POWTEC.2017.01.059
Zhang, R., Panesar, D.K., 2019. Sulfate resistance of carbonated ternary mortar blends: Portland cement, reactive MgO and supplementary cementitious materials. J Clean Prod 238, 117933. https://doi.org/10.1016/J.JCLEPRO.2019.117933
Zong, Z., Cai, G., Tabbara, M., Chester Upham, D., 2023a. CO2-negative fuel production using low-CO2 electricity: Syngas from a combination of methane pyrolysis and dry reforming with techno-economic analysis. Energy Convers Manag 277, 116624. https://doi.org/10.1016/J.ENCONMAN.2022.116624
Zong, Z., Hankins, N., Parveen, F., 2023b. The Application of Nanofiltration for Water Reuse in the Hybrid Nanofiltration-Forward Osmosis Process, in: Nanofiltration for Sustainability. CRC Press, pp. 153–170.
Zong, Z., Koers, N., Cai, G., Upham, D.C., 2024. CO2-to-methanol: Economic and environmental comparison of emerging and established technologies with dry reforming and methane pyrolysis. Chemical Engineering Journal 150274. https://doi.org/10.1016/J.CEJ.2024.150274